Instrumentation Technique for Measuring Six Degrees of Freedom Head Kinematics in Impact Conditions using Six-Accelerometers and Three-Angular Rate Sensors (6aω Configuration) on a Lightweight Tetrahedron Fixture

Yun-Seok Kang
Injury Biomechanics Research Center, The Ohio State University
USA

Kevin Moorhouse
National Highway Traffic Safety Administration, Vehicle Research & Test Center
USA

John H. Bolte IV
Injury Biomechanics Research Center, The Ohio State University
USA

Paper Number 15-0288

ABSTRACT

The ability to measure six degree of freedom head kinematics in impact conditions (i.e. motor vehicle crashes and sport activities) plays an important role in injury assessment of the head/neck complex. Potential accuracy of head instrumentation schemes have recently been improved by using advanced angular rate sensors, so in this study an instrumentation technique for obtaining accurate head kinematics in impact conditions using an external fixture is proposed and validated. The methodology proposed in this study utilizes six accelerometers and three angular rate sensors (6aω) on a lightweight tetrahedron fixture (t6aω) originally designed for measuring head kinematics of post mortem human surrogates (PMHS) in car crash scenarios using a nine accelerometer array package (NAAP) configuration (tNAAP). A Hybrid III 50th percentile male anthropomorphic test device (ATD) head containing an internal nine accelerometer array package (iNAAP) was used to validate the t6aω method proposed in this study. The t6aω instrumentation was installed on a tetrahedron fixture which was attached externally to the Hybrid III ATD head, tested in direct contact tests of various severities, and then compared to data measured from the iNAAP of the Hybrid III ATD head which provided the kinematics gold standard to validate the proposed technique. Results indicate that angular acceleration obtained from the t6aω scheme was comparable to that determined from the iNAAP scheme in the head impact conditions, showing normalized root mean squared deviation (NRMSD) values less than 5%. Transformed linear acceleration from the t6aω to the center of gravity (CG) of the Hybrid III ATD head was also comparable to acceleration measured directly from the accelerometers at the CG, exhibiting less than 5% NRMSD. Accurate angular acceleration and velocity are important to obtain accurate transformed acceleration. Since the t6aω angular acceleration component of the transformed linear acceleration at an inaccessible point was shown to have equivalent accuracy to iNAAP (less than 5% error), and the angular velocity component of t6aω instrumentation should be more accurate than the tNAAP scheme (since it is directly measured by the ARS as opposed to using numerical integration as in tNAAP), the t6aω scheme should yield more accurate transformed linear acceleration at an inaccessible location than the tNAAP scheme. The proposed instrumentation should aid in the development and evaluation of head, neck and brain injuries in future testing.

INTRODUCTION

Numerous measurement techniques for head kinematics in motor vehicle crashes and sports activities have been developed and evaluated [1-9], and the accuracy of angular kinematics, in particular, has been a challenge in developing these instrumentation techniques [1-4, 7]. The most frequent method to obtain accurate six degrees of freedom (6DOF) head kinematics is to use the nine accelerometer array (3-2-2-2) package (NAAP), in which angular acceleration can be calculated from simple algebraic equations [1]. Although the NAAP is capable of measuring angular acceleration accurately, single and double numerical integrations are required to obtain angular

velocity and displacement, which can particularly cause issues with the accuracy of the resulting displacement [5, 7]. Therefore, with the advent and availability of more advanced angular rate sensors (ARS), ARS combined with accelerometers have been recently employed to provide even more accurate angular velocity and displacement [5], since angular acceleration can still be obtained from algebraic equations, while angular velocity is directly measured from the ARS [7]. Therefore, six accelerometers and three ARS (6aω) should theoretically be capable of measuring more accurate 6DOF kinematics than NAAP, and this has been demonstrated for sensors installed inside an ATD head (i6aω versus iNAAP where "i" stands for internal) [7].

In order to measure 6DOF kinematics of the head of post mortem human surrogates (PMHS), an external fixture is typically used, and should be lightweight and stable against structural vibration. Previous studies evaluating head and brain injuries have used various external fixtures with nine accelerometers (NAAP) installed, such as a triangular pyramidal fixture [10] and a tetrahedral fixture [11]. Although the i6aω scheme has been validated inside a Hybrid III iNAAP head [7], its integrity with a lightweight/small external fixture should also be validated. Therefore, the objective of this study is to propose and validate a 6aω scheme installed on a lightweight tetrahedron fixture (t6aω, where "t" stands for tetrahedron).

METHODS

6aω Scheme on a Lightweight Tetrahedron Fixture

An external tetrahedron fixture, similar to the one developed and validated (including its structural integrity and stability) by Yoganandan et al. [10], was utilized in this study. The t6aω scheme was implemented as shown in Figure 1. The edge length of the tetrahedron is approximately 6 cm, while the mass of the fixture is 72 grams without sensors and 96 grams with sensors attached. In order to obtain algebraic equations for angular acceleration of the t6aω scheme, the acceleration at each corner point (points A-B-C shown in Figure 1b) with respect to a body fixed coordinate system on the tetrahedron fixture was derived as Eqs (1) – (3).

$$a_{az'} = a_{0z'} + \omega_{x'}\,\omega_{z'}\rho_{ax'} - \dot{\omega}_{y'}\rho_{ax'} \tag{1}$$

$$a_{bx'} = a_{0x'} + \omega_{x'}\,\omega_{y'}\rho_{by'} - \dot{\omega}_{z'}\rho_{by'} \tag{2}$$

$$a_{cy'} = a_{0y'} + \omega_{y'}\,\omega_{z'}\rho_{cz'} - \dot{\omega}_{x'}\rho_{cz'} \tag{3}$$

where,
$\dot{\omega}$: angular acceleration in the body fixed frame
a : acceleration measured from accelerometers at each location
ω : angular velocity measured from ARS
ρ : distance between accelerometers at vertex and accelerometers at points A, B, and C

Eqs (1) – (3) can now be expressed in terms of the angular accelerations, which are the only unknown variables under the proposed t6aω configuration, as in Eqs (4) – (6):

$$\dot{\omega}_{x'} = (a_{0y'} - a_{cy'}) / \rho_{cz'} + \omega_{ay'}\omega_{bz'} \tag{4}$$

$$\dot{\omega}_{y'} = (a_{0z'} - a_{az'}) / \rho_{ax'} + \omega_{cx'}\omega_{bz'} \tag{5}$$

$$\dot{\omega}_{z'} = (a_{0x'} - a_{bx'}) / \rho_{by'} + \omega_{cx'}\omega_{ay'} \tag{6}$$

The detailed procedure for deriving the kinematic equations with respect to the body fixed frame for the t6aω scheme is described in a previous study [7].

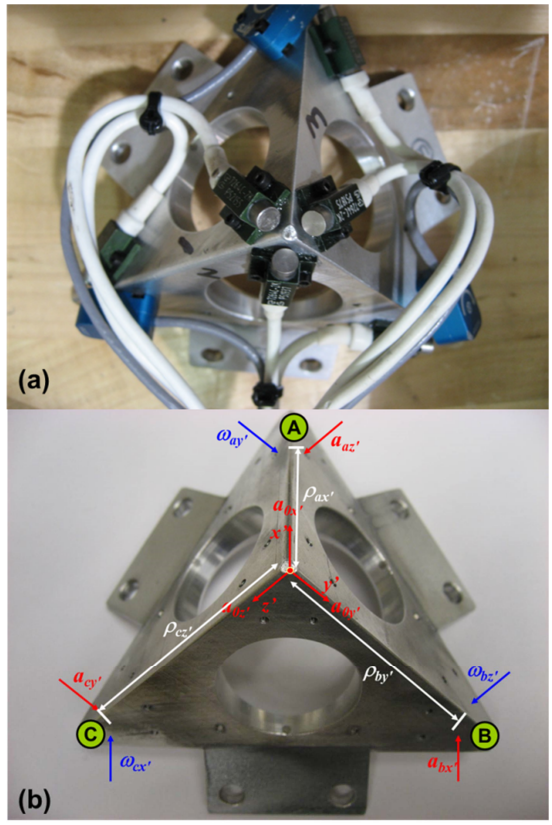

Figure 1. (a) An external fixture with 6aω scheme and (b) body fixed coordinate system embedded on the tetrahedron fixture.

Test Configuration and Instrumentation

Thirteen head impact tests were conducted to validate the proposed external instrumentation in a direct impact condition that usually yields high peak, short duration responses. The Hybrid III head/neck was fixed to an adjustable height table and a hydraulic ram impactor was used to deliver a severe head impact. The lower neck of the Hybrid III was fixed to the table after being rotated 30 degrees about the z direction according to SAE J211 (SAE, 2007), as shown in Figure 2, such that the impactor could collide with the head antero-laterally. The body fixed frame (x-y-z) on the Hybrid III head was defined as shown in Figure 2. In order to produce various severities and head injury criteria (HIC) values, the head was struck by the impactor without padding for five tests and with padding for eight tests. For the padded condition a one inch thick piece of gray "Ensolite SCC" foam was affixed to the head at the impact location. The Hybrid III iNAAP head was instrumented with nine accelerometers (Endevco 7264C 2K), while the t6aω scheme installed on the tetrahedron fixture was composed of six accelerometers (Endevco 7264C 2K) and three ARS (DTS ARS-18K). In addition to the t6aω scheme, a t3aω scheme on the tetrahedron fixture was also evaluated in this study. The t3aω scheme was composed of the three accelerometers at the origin (i.e. vertex of the fixture) and the three ARS at points A-B-C shown in Figure 1. Accuracy of the external instrumentation could be affected by any relative movement between the fixture and the head. To reduce the risk of relative motion, the tetrahedron fixture was screwed into the skull cap using six screws, as shown in Figure 2.

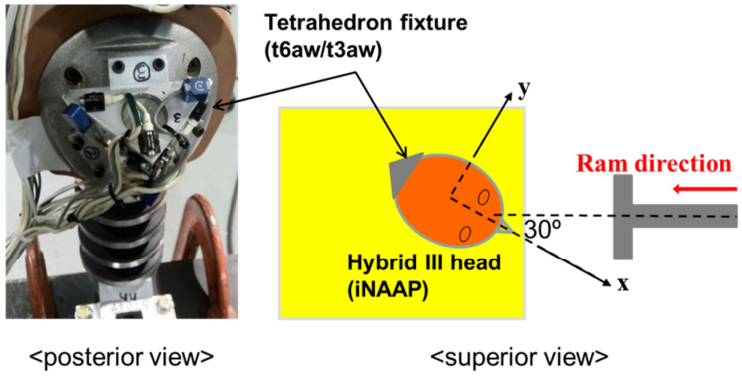

Figure 2. Head impact test configuration

Data Analyses

Data was sampled at 20,000 Hz. The consistency of the data measured from the accelerometers of the iNAAP was inspected by SIMon (version 4.0, NHTSA), which checked the integrity of the accelerometers, including instances of sensor malfunction and incorrect sensitivity [13, 14]. A 4th-order Butterworth low pass filter corresponding to appropriate SAE J211 channel filter classes (CFC) was applied to the data. For the iNAAP and t6aω schemes, the data recorded from the accelerometers and ARS were filtered at 1650 Hz (CFC1000). The angular velocity for the t3aω scheme was first filtered at 300 Hz (CFC180) and then numerically differentiated to obtain angular acceleration. Angular acceleration for the iNAAP was calculated by employing the procedure proposed by Padgaonkar et al. [1], while that for the t6aω was determined using Eqs (4) – (6). The kinematic data relative to the body fixed coordinate system on the external fixture was transformed to the body fixed coordinate system on the Hybrid III head using the procedure described by Kang et al. [7]. Origin locations and initial orientation of the body fixed coordinates for both the external fixture and the Hybrid III head were determined by digitizing points on the fixture and the head using a Faro arm device (Faro Arm Technologies, Lake Mary, FL). The normalized root mean squared deviation (NRMSD) shown in Eq (7) was used for quantitative evaluation of the proposed scheme. The NRMSD provided an average percent error over time between the iNAAP (i.e. gold standard) and kinematic data (linear acceleration and angular acceleration) obtained from the t6aω and t3aω. In addition to the NRMSD, percent differences of the peak values between the iNAAP and t6aω/t3aω schemes were also calculated since most injury criteria rely upon peak values.

$$NRMSD = \frac{\sqrt{\frac{1}{n}\sum_{i=0}^{n}(Y_i - Y_i')^2}}{Y'_{\max} - Y'_{\min}} \tag{7}$$

where:

- n is the total number of data points
- *Y'max* and *Y'min* represent the maximum and minimum values of the gold standard.
- *Yi* and *Y'i* are the ith data point obtained from the instrumentation scheme being evaluated and the ith data point obtained from the gold standard, respectively.

The angular velocity for the iNAAP was also computed using a single numerical integration, and then transformed to the coordinate system on the tetrahedron fixture so it could be compared to the angular velocity

directly measured on the tetrahedron by the ARS. For this evaluation the directly measured ARS were deemed as the gold standard for NRMSD calculation.

RESULTS

Three dimensional head motion was generated to validate the proposed instrumentation technique for measuring six degrees of freedom kinematics. Various impact severities were created randomly, ranging from HIC15 values of 319 to 1820. Many studies have looked at resultant linear and/or angular acceleration in their validation studies for instrumentation techniques [5, 6, 8, 10, 15, 16], likely due to the fact that transformation errors can be minimized by using the resultant acceleration. However, considering linear and angular kinematics in each component direction (x, y, and z) has been shown to be important in the prediction of brain injury [17]. Therefore, in this study linear and angular acceleration with respect to the body fixed frame on the tetrahedron fixture was transformed to the head coordinate system in x, y, and z axes at the center of gravity (CG) (Figure 2). When transforming the kinematics to the head CG coordinate system there can be some inherent transformation errors due to digitization of the tetrahedron fixture and ATD landmarks (e.g. OC joint and peripheral CG point). However, these transformation errors are likely to be small since both the tetrahedron and the ATD head have well-defined geometries. Figure 3 shows the linear and angular acceleration in x, y, and z axes for HImpact13, which resulted in a HIC15 value of 1820 (Table 1). NRMSD values were calculated for the first 40 ms after head contact for each test. Despite inherent transformation errors, the t6aω scheme yielded an average NRMSD of 1.8 ± 1.0% for the linear acceleration and 3.4 ± 0.9% for the angular acceleration, while the t3aω produced an average NRMSD of 5.6 ± 5.6% for the linear acceleration and 5.4 ± 1.4% for the angular acceleration for all thirteen tests (Tables 1 and 2). For the average peak value differences, the t6aω scheme yielded an average 5.3 ± 4.1% for the linear acceleration, 5.0 ± 4.8% for the angular acceleration and 2.4 ± 1.0% for HIC_{15}, while the t3aω produced an average 16.0 ± 21.7% for the linear acceleration, 14.0 ± 15.6% for the angular acceleration and 1.6 ± 1.3% for HIC_{15} in all thirteen tests.

When evaluating the NRMSD values or peak value differences in Tables 1 and 2 it is important to consider the importance and/or magnitude of the signal being assessed, because in many cases the high percentage differences are simply a result of a low signal magnitude dominated by noise. Therefore, linear accelerations with a magnitude greater than 100g were highlighted in green in Table 1, and average NRMSD and peak value differences were calculated only using the highlighted linear accelerations with sufficient magnitude. Average NRMSD and peak value differences calculated in this manner were reduced for the t6aw configuration: 1.0 ± 0.8% for NRMSD and 2.9 ± 3.7% for peak value differences. The t3aw configuration showed even greater reduction in NRMSD and peak values differences: 1.4 ± 1.3% for NRMSD and 5.1 ± 6.6% for peak value differences.

Similarly in Table 2, angular accelerations with a magnitude greater than 3000 rad/s^2 were highlighted in yellow and the mean and standard deviation for only highlighted angular accelerations were calculated. Average NRMSD and peak value differences using only the highlighted angular accelerations were reduced to 3.1 ± 0.5% NRMSD and 3.7 ± 4.4% peak value differences for the t6aw, and 4.6 ± 1.2% NRMSD and 5.4 ± 6.5% peak value differences for the t3aw.

NRMSD and peak value differences for angular velocities are also shown in Table 2, and angular velocities with a magnitude greater than 1000 deg/s are highlighted in green. The average NRMSD for all thirteen tests was 4.6 ± 1.1%, while the average including only highlighted values was 5.0 ± 1.2%. For the average peak value differences in angular velocity, both mean values were less than 5% (4.7 ± 2.0% for all thirteen values and 4.3 ± 1.3% for only the highlighted values).

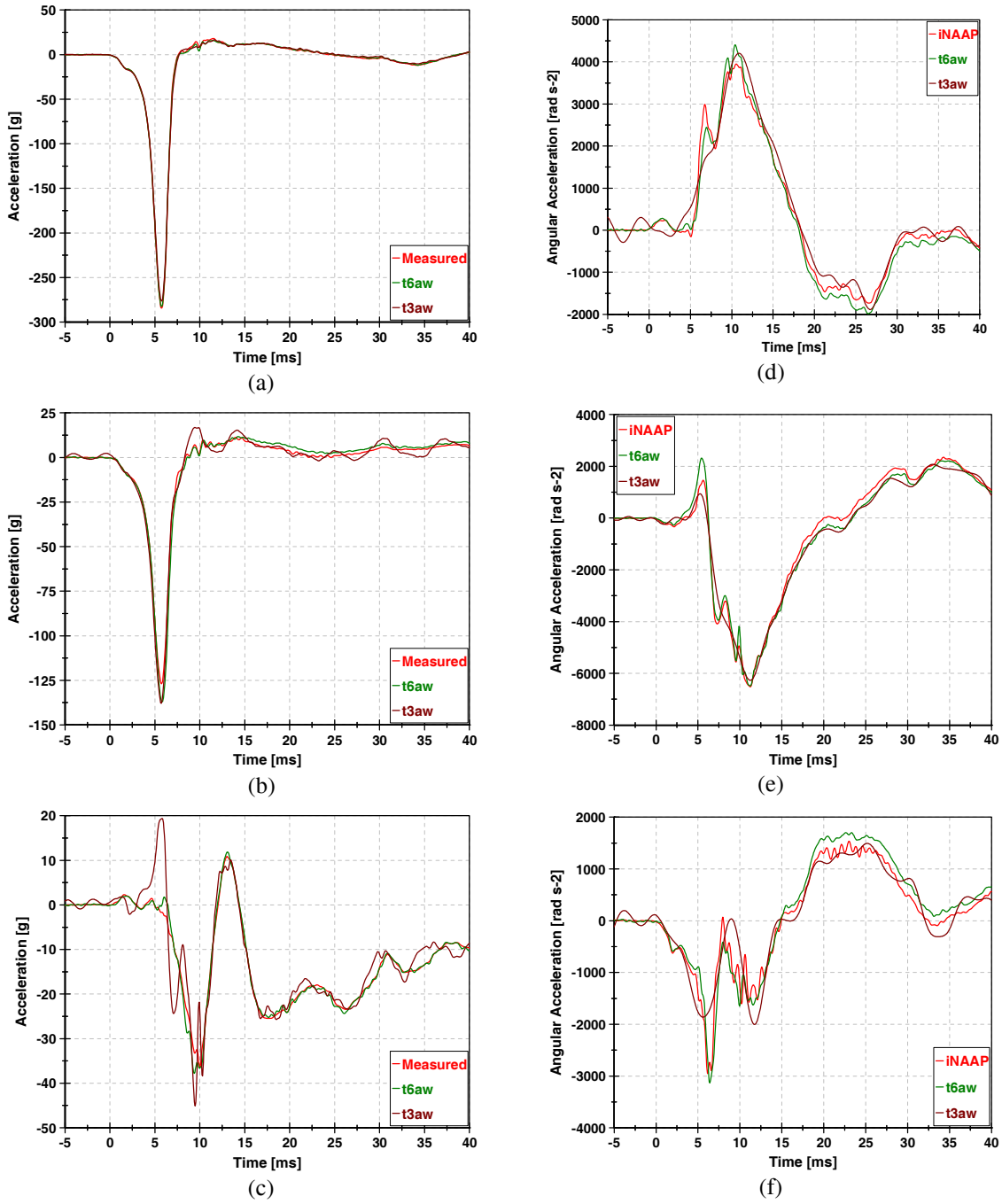

Figure 3. Kinematics in HImpact13: linear acceleration in (a) x direction, (b) y direction, (c) z direction and angular acceleration in (d) x direction, (e) y direction, (f) z direction
Filter class: CFC1000 for accelerometers in all three schemes, CFC1000 for ARS in t6aω, and CFC180 for ARS in t3aω due to numerical differentiation

Table 1.
NRMSD and peak value percent differences (t6aω vs. NAAP and t3aω vs. NAAP) for linear acceleration at CG and HIC_{15}
Gold standard: measured acceleration at CG
Highlighted cells: Acceleration > 100g

	Pad	HIC_{15}	HIC_{15} Peak difference (%)		Axes	Linear acceleration NRMSD (%)		Linear acceleration Peak difference (%)	
			t6aω	t3aω		t6aω	t3aω	t6aω	t3aω
HImpact01	No	381	2.9	3.7	x	0.4	0.7	1.4	1.1
					y	2.1	4.4	6.9	20.7
					z	3.1	21.3	4.3	6.7
HImpact02	No	633	1.9	1.6	x	0.4	0.8	2.1	2.8
					y	2.0	4.1	11.1	22.5
					z	3.1	17.6	15.9	128.2
HImpact03	No	934	0.7	0.3	x	0.4	0.7	0.2	1.4
					y	1.9	4.3	2.9	20.1
					z	2.5	15.8	9.3	21.2
HImpact04	No	1001	1.7	2.8	x	0.5	0.5	0.4	1.0
					y	1.9	4.0	7.5	21.3
					z	2.5	12.6	10.0	51.6
HImpact05	No	1059	2.2	2.6	x	0.6	0.8	0.2	0.7
					y	1.8	3.8	6.4	16.4
					z	1.8	13.1	4.1	32.2
HImpact06	Yes	319	4.4	4.1	x	0.5	0.7	0.4	1.2
					y	3.0	4.5	9.7	14.6
					z	3.4	13.7	6.4	12.6
HImpact07	Yes	543	2.9	0.2	x	0.6	0.7	0.4	0.9
					y	2.5	3.0	8.0	9.7
					z	2.1	10.3	4.9	9.8
HImpact08	Yes	846	2.7	1.3	x	0.7	0.8	1.9	2.9
					y	2.3	2.6	7.6	8.2
					z	2.4	8.8	9.1	29.8
HImpact09	Yes	1153	2.9	1.4	x	0.4	0.6	0.1	1.1
					y	2.2	2.8	8.2	9.7
					z	2.1	8.9	5.5	23.9
HImpact10	Yes	1183	3.0	0.3	x	0.5	0.6	0.5	1.6
					y	2.4	3.0	8.1	8.2
					z	2.3	9.7	4.9	20.8
HImpact11	Yes	1421	3.2	0.7	x	0.5	0.6	0.8	2.1
					y	2.4	2.5	9.9	10.5
					z	2.8	8.5	3.9	14.3
HImpact12	Yes	1432	1.0	0.2	x	0.5	0.7	0.6	2.7
					y	2.3	4.9	10.4	24.7
					z	4.0	14.0	11.9	29.2
HImpact13	Yes	1820	1.8	1.5	x	0.4	0.6	0.6	2.8
					y	2.0	2.4	8.0	8.7
					z	2.0	8.4	3.8	23.9
Total mean (SD)	N/A	979 (439)	2.4 (1.0)	1.6 (1.3)	N/A	1.8 (1.0)	5.6 (5.6)	5.3 (4.1)	16.0 (21.7)
Highlighted mean (SD)	N/A	N/A	N/A	N/A	N/A	1.0 (0.8)	1.4 (1.3)	2.9 (3.7)	5.1 (6.6)

Table 2.
NRMSD and peak value percent differences for angular velocity (NAAP vs. ARS) and angular acceleration (t6aω vs. NAAP and t3aω vs. NAAP)
Gold standards: ARS for angular velocity; NAAP for angular acceleration
Highlighted cells: angular velocity > 1000 deg/s; angular acceleration > 3000 rad/s^2

	Pad	HIC_{15}	Axes	Angular velocity		Angular acceleration			
				NRMSD (%)	Peak difference (%)	NRMSD (%)		Peak difference (%)	
				iNAAP	iNAAP	t6aω	t3aω	t6aω	t3aω
HImpact01	No	381	x	3.5	4.7	3.5	8.2	3.4	9.9
			y	3.9	4.0	3.3	7.1	1.7	5.7
			z	5.2	12.1	2.2	5.9	2.5	40.0
HImpact02	No	633	x	3.9	2.0	3.8	8.2	3.8	8.6
			y	3.7	3.6	3.0	4.9	0.1	3.6
			z	4.5	8.7	3.1	6.0	14.2	29.3
HImpact03	No	934	x	3.6	3.8	2.5	5.5	10.7	9.6
			y	4.0	5.5	2.1	4.5	1.1	0.0
			z	3.6	6.0	3.1	6.3	6.1	41.6
HImpact04	No	1001	x	3.8	3.9	3.7	6.8	2.1	1.5
			y	4.6	4.2	2.8	4.4	0.7	3.7
			z	3.9	7.0	3.2	6.7	24.0	30.9
HImpact05	No	1059	x	4.0	3.2	3.4	7.3	4.2	2.3
			y	4.7	4.9	3.0	5.5	1.8	0.0
			z	3.9	8.5	3.1	5.8	3.1	50.5
HImpact06	Yes	319	x	4.0	2.9	2.9	3.8	9.0	1.8
			y	5.2	4.3	4.6	7.6	1.6	4.1
			z	4.0	4.2	6.4	6.4	2.2	3.3
HImpact07	Yes	543	x	3.9	4.0	3.2	5.5	6.2	1.2
			y	5.7	4.0	2.6	3.4	0.9	0.9
			z	3.2	4.2	4.5	5.4	5.0	36.3
HImpact08	Yes	846	x	4.7	7.0	3.0	4.6	9.8	9.9
			y	5.9	5.4	2.5	3.4	0.8	1.2
			z	4.1	3.4	4.6	4.5	9.5	31.9
HImpact09	Yes	1153	x	5.0	5.1	3.1	3.8	8.9	6.6
			y	6.3	3.8	2.8	3.4	0.7	1.2
			z	3.6	3.5	4.9	5.5	4.8	26.3
HImpact10	Yes	1183	x	5.1	4.3	3.2	4.5	4.2	8.8
			y	6.7	6.8	2.9	3.5	1.0	3.0
			z	3.7	1.8	5.3	6.1	6.7	34.7
HImpact11	Yes	1421	x	5.7	3.9	3.7	5.0	7.9	8.6
			y	7.3	5.6	3.1	3.6	0.4	0.5
			z	4.3	3.8	5.1	5.2	3.5	23.8
HImpact12	Yes	1432	x	3.8	3.6	3.9	6.5	2.4	6.4
			y	4.3	4.1	3.0	4.2	1.6	5.5
			z	4.1	6.9	2.7	5.6	10.2	50.0
HImpact13	Yes	1820	x	5.8	3.9	3.1	4.6	11.6	6.4
			y	7.3	4.5	2.6	3.5	0.5	3.8
			z	4.1	1.3	4.6	6.2	6.2	32.1
Total mean (SD)	N/A	979 (439)	N/A	4.6 (1.1)	4.7 (2.0)	3.4 (0.9)	5.4 (1.4)	5.0 (4.8)	14.0 (15.6)
Highlighted mean (SD)	N/A	N/A	N/A	5.0 (1.2)	4.3 (1.3)	3.1 (0.5)	4.6 (1.2)	3.7 (4.4)	5.4 (6.5)

DISCUSSION

Various filtering classes for the instrumentation have been suggested to yield accurate head kinematics [2, 5, 7, 10, 11, 18]. The same filtering class (1650 Hz cutoff frequency, CFC1000) was applied to the accelerometers and ARS for both the t6aω (all six accelerometers and three ARS) and iNAAP (nine accelerometers) schemes. However, the t3aω scheme required a different filtering class due to numerical differentiation of the data measured from the angular rate sensors [2, 5, 7]. In order to determine the most appropriate filtering class for numerical differentiation in the t3aω scheme, different filtering cut-off frequencies were applied to the most severe impact tests: HImpact05 (with no padding and HIC15 value of 1059) and HImpact13 (with padding and HIC15 value of 1820) shown in Figure 4(a) and 4(b), respectively. Representative traces for both HImpact 05 and 13 are presented in Figure 4(c) and 4(d), respectively, where it can be seen that inaccuracies were inherent in the 100 Hz cut off frequency due to excessive signal attenuation, and also in the 500 Hz cut off frequency due to excessive noise. The NRMSD and peak value differences of the resultant angular acceleration between the iNAAP and t3aω were smallest at 300 Hz (CFC180) in the unpadded test (Figure 4a), consistent with what previous studies have used [4, 5]. Although the peak values were still smallest at 300 Hz in the padded test (Figure 4b), the NRMSD values were smallest at 400 Hz. For the most part, NRMSD and peak value differences in the padded test (HImpact13) were smaller than those in the unpadded test (HImpact05). Numerical differentiation errors in the t3aω scheme seem to be reduced in padded head impacts.

In a rigid body, the accuracy of the measured angular acceleration at a remote point affects the accuracy of the transformed linear acceleration at other locations which may be inaccessible (e.g., center of gravity of the head), because transformed linear acceleration is a function of both angular velocity and angular acceleration (Eqs 1 – 3). Therefore, accurate angular acceleration and velocity are important to obtain accurate transformed acceleration. Since the t6aω angular acceleration component of the transformed linear acceleration at an inaccessible point was shown to have equivalent accuracy to iNAAP, and the angular velocity component of t6aω instrumentation should be more accurate since it is directly measured by the ARS (as opposed to using numerical integration as in tNAAP), the t6aω should theoretically yield more accurate transformed linear acceleration at an inaccessible location than tNAAP.

Both 6aω and NAAP schemes use algebraic equations to compute angular acceleration [1, 7], which is numerically more stable and accurate than using nonlinear ordinary differential equations [19] and numerical differentiation of ARS [2, 5]. The NRMSD and peak value differences for the angular velocity determined from iNAAP were 4.6% and 4.7% (Table 2), which is generally acceptable, but the t6aω scheme should theoretically provide the most accurate six degrees of freedom head kinematics since the angular velocity is measured directly. The 6aω scheme should also provide more accurate angular displacement, and thus the most accurate six degrees of freedom head kinematics, both when installed inside an ATD head and when installed on an external fixture mounted to the outside of the head.

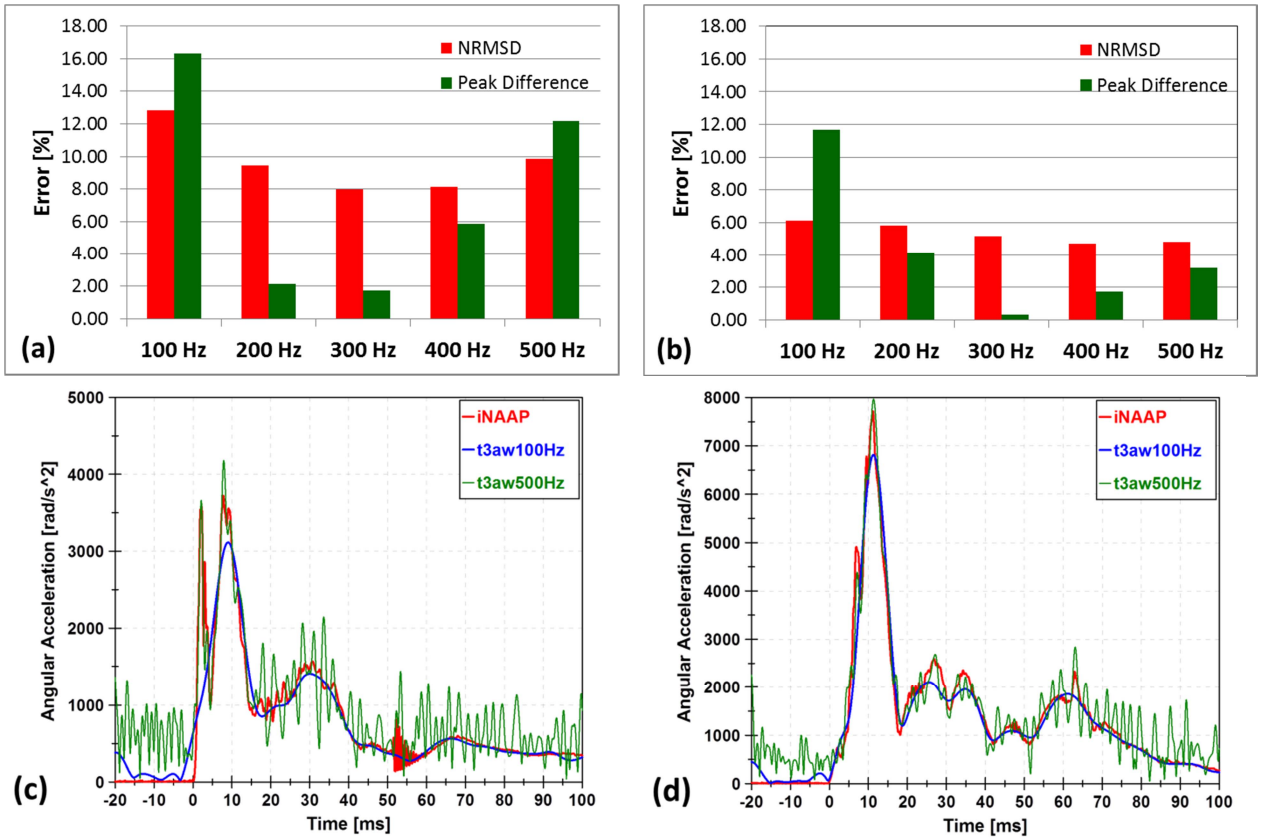

Figure 4. NRMSD and peak difference of the angular acceleration between iNAAP and t3aω using different filtering classes: (a) HImpact05 (no pad impact), (b) HImpact13 (pad impact), (c) representative traces for HImpact05 (no pad impact), and (d) representative traces for HImpact13 (pad impact)

CONCLUSIONS

Six accelerometers and three angular rate sensors (6aω) installed on an external tetrahedron fixture (t6aω) were proposed and validated on a Hybrid III nine accelerometers array package (NAAP) head. Validation tests were conducted in various HIC15 levels (HIC15 of 319 to 1820). Quantitative comparison using the NRMSD and peak percent difference were made between each scheme evaluated (t6aω and t3aω) and the relevant gold standard (iNAAP). The proposed t6aω method appears to be capable of measuring accurate 6 DOF kinematics of the head in any severity of impact conditions. The results exhibited NRMSD less than 4% and peak percent difference less than 6% for both linear and angular acceleration. The proposed instrumentation should aid in the development and evaluation of head, neck and brain injuries in future testing.

ACKNOWLEDGMENTS

The authors would like to thank Jim Stricklin and David Hyder from the Transportation Research Center, Inc. for their considerable support during test days.

REFERENCES

[1] Padgaonkar, A., Krieger, K., King, A., 1975. Measurement of angular acceleration of a rigid body using linear accelerometers. Journal of Applied Mechanics 42, 552–556.
[2] Laughlin, D.R., 1989. A magnetohydrodynamic angular motion sensor for anthropomorphic test device instrumentation. Stapp Car Crash Journal, 33, 43 – 77.
[3] Nusholtz, G.S., 1993. Geometric methods in determining rigid-body dynamics. Exp. Mech. 33, 153–158.
[4] Martin, P.G., Hall, G.W., Crandall, J.R., Pilkey, W.D., Chou, C.C., Fileta, B.B., 1997. Measurement Techniques for Angular Velocity and Acceleration in an Impact Environment. SAE Paper 970575.
[5] Martin, P.G., Hall, G.W., Crandall, J.R., Pilkey, W.D., 1998. Measuring the Acceleration of a Rigid Body. Shock and Vibration 5, 211-224.
[6] Hanlon, E., Bir, C., 2010. Validation of a wireless head acceleration measurement system for use in soccer play. J. Appl. Biomech. 26, 424–31.
[7] Kang, Y.-S., Moorhouse, K., Bolte, J.H., 2011. Measurement of six degrees of freedom head kinematics in impact conditions employing six accelerometers and three angular rate sensors (6aω configuration). J. Biomech. Eng. 133, 111007.
[8] Rowson, S., Beckwith, J.G., Chu, J.J., Leonard, D.S., Greenwald, R.M., Duma, S.M., 2011. A six degree of freedom head acceleration measurement device for use in football. J. Appl. Biomech. 27, 8–14.
[9] Allison, M., Kang, Y., Maltese, M., Bolte, J., 2013. Validation of a Helmet-Based System to Measure Head Impact Biomechanics in Ice Hockey. Medicine and Science in Sports and Exercise, DOI: 10.1249/MSS.0b013e3182a32d0d.
[10] Yoganandan, N., Zhang, J., Pintar, F. A, Liu, Y., 2006. Lightweight low-profile nine-accelerometer package to obtain head angular accelerations in short-duration impacts. J. Biomech. 39, 1347–54.
[11] Hardy, W.N., Foster, C., Mason, M., Yang, K., King, A., Tashman, S., 2001. Investigation of Head Injury Mechanism Using Neutral Density Technology and High-Speed Biplanar X-ray. Stapp Car Crash Journal, 45, 337-368.
[12] SAE, 2007. Instrumentation for impact test, Part 1: Electronic instrumentation, SAE J211/1, Society of Automotive Engineers.
[13] Takhounts, E.G., Eppinger, R.H., Campbell, J.Q., Tannous, R.E., Power, E.D., Shook, L.S., 2003. On the Development of the SIMon Finite Element Head Model. Stapp Car Crash Journal, 47, 107-33.
[14] Takhounts, E.G., Hasija, V., Eppinger, R. H., 2009. Analysis of 3D Rigid Body Motion Using The Nine Accelerometer Array and the Randomoly Distributed in-plane Accelerometer Systems. In Proceedings of International Technical Conference on the Enhanced Safety of Vehicle, Stuttgart, Germany.
[15] Crisco, J.J., Chu, J.J., Greenwald, R.M., 2004. An Algorithm for Estimating Acceleration Magnitude and Impact Location Using Multiple Nonorthogonal Single-Axis Accelerometers. J. Biomech. Eng. 126, 849.
[16] Duma, S.M., Manoogian, S.J., Bussone, W.R., Brolinson, P.G., Goforth, M.W., Donnenwerth, J.J., Greenwald, R.M., Chu, J.J., Crisco, J.J., 2005. Analysis of real-time head accelerations in collegiate football players. Clin. J. Sport Med. 15, 3–8.
[17] Takhounts, E.G., Craig, M.J., Moorhouse, K., McFadden, J., 2013. Development of Brain Injury Criteria (BrIC). Stapp Car Crash Journal, 57, 243-66.
[18] Hardy, W.N., Mason, M., Foster, C.D., Shah, C.S., Kopacz, J.M., Yang, K.H., King, A.I., 2007. A Study of the Response of the Human Cadaver Head to Impact. Stapp Car Crash Journal, 51, 17-80.
[19] Becker, E., Willems, G., 1975. An experimentally validated 3-D inertial tracking package for application in biodynamic research. Stapp Car Crash Journal 19, 899-930.